

See discussions, stats, and author profiles for this publication at: <https://www.researchgate.net/publication/231341090>

# Molecular Modeling of Dimetal Systems. Dimolybdenum Quadruple Bonds

ARTICLE *in* INORGANIC CHEMISTRY · APRIL 1995

Impact Factor: 4.76 · DOI: 10.1021/ic00112a007

---

CITATIONS

9

---

READS

6

2 AUTHORS, INCLUDING:



Jan Boeyens

University of Pretoria

311 PUBLICATIONS 4,034 CITATIONS

SEE PROFILE

## Molecular Modeling of Dimetal Systems. Dimolybdenum Quadruple Bonds

Jan C. A. Boeyens\* and Françoise M. M. O'Neill†

Department of Chemistry, University of the Witwatersrand, P.O. WITS 2050, Johannesburg, South Africa

Received November 4, 1993<sup>®</sup>

The concept of quadruple bonding at a dimetal center has been used very successfully to account for the eclipsed conformation of unbridged dimers, contrary to steric demands. The situation is more complicated in the case of bridged dimers with sterically dictated eclipsed structures. Electronic factors operating through bridging, as well as axial, ligands have such a serious influence on observed bond lengths and conformations that, in this case, the effective bond order of the formally quadruply-bonded systems is moot. A strategy is defined whereby different factors contributing to the observed trends can be separately assessed. This is achieved by systematic molecular modeling of a large number of Mo<sub>2</sub> and Cr<sub>2</sub> derivatives to establish a general mathematical relationship among strain-free bond lengths, force constants, and bond orders. The modeling of compounds with Mo<sup>4</sup>–Mo bonds and well-refined crystallographic structures is reported here. All structural details independent of the dimolybdenum bond are simulated in terms of a transferable force field. Simulation of the dimetal-bond properties is then achieved by trial-and-error procedures, in terms of a family of matched pairs of harmonic force constant ( $k_r$ ) and characteristic bond length ( $r_0$ ), for each bond. These solution curves have different slopes for bridged and unbridged compounds, and they intersect within a sufficiently small region to define a characteristic solution pair of  $k_r = 4.07$  mdyn Å<sup>-1</sup> and  $r_0 = 2.02$  Å. A torsional twist through the angle  $\chi$ , away from eclipsing, is calculated to reduce the  $\delta$  stabilization by a factor of  $\cos 2\chi$  from a maximum of 50 kJ mol<sup>-1</sup> at  $\chi_0$ .

## Introduction

Dimetal centers present a special challenge in molecular modeling because of the extreme variability of the bond length within families of theoretically constant bond order. The most striking example is provided<sup>1</sup> by the Cr(II)–Cr(II) bonds in compounds like Cr<sub>2</sub>(X<sup>^</sup>Y)<sub>4</sub>L<sub>2</sub> and their response to axial ligation. It is not clear if the inductive effect of the bridging X<sup>^</sup>Y ligand has a more or a less important influence on the bond length than the nature of the axial ligand, L. The situation is invariably further complicated by steric interactions. In any systematic study of the problem it is therefore essential to first eliminate the steric complication, and this can be achieved effectively by the method of molecular mechanics.<sup>2</sup>

The strategy is to define a force field that faithfully simulates the known crystallographic structure. Since all nonbonded interactions are simulated separately, the final force-field parameters, characterizing all other interactions, would reflect electronic effects only, if the parameters for nonbonded terms are unique and known with certainty. We tried to simulate this condition by the strict requirement of considering only those structures for which the general force field correctly reproduces all observed features and internal parameters, apart from the dimetal bond, in precise detail. One of these parameters is a strain-free bond length ( $r_0$ ), and it is suggested to be a more reliable measure of the electronic factors, responsible for trends in bond order, than observed bond lengths, which represent a balance between steric and electronic factors. It is therefore not surprising that attempts to interpret the effects directly in terms of uncorrected bond lengths are rather inconclusive.<sup>1</sup>

Unfortunately, use of characteristic force-field parameters as a measure of strain-free bond lengths is also not without

problems. Simulation of a chemical bond requires at least two mutually dependent parameters, usually  $r_0$  and a force constant,  $k_r$ . Unless one of these is established independently a whole family of solution curves,  $\{k_r, r_0\}$  exists,<sup>3</sup> effectively masking the bond order. Only when a unique pair has been identified for a given bond, is it possible to explore properties such as barriers to rotation by computer-driven rotation, linked to molecular mechanics minimization at each step, in order to measure the bond order.

## The Bond-Order Concept

As the most important theoretical concept to be analyzed in this study, the notion of bond order needs clear definition at the outset.

The term M–M bond order is used most commonly only to specify the number of electron pairs thought to play a significant part in holding the pair of metal ions together. Based on bond length, conformation, electronic and vibrational absorption spectroscopy, theoretical calculations, and internal consistency, the evidence for multiple bonding in certain compounds is overwhelming. Such is the case for the quadruple [Mo<sub>2</sub>Cl<sub>8</sub>]<sup>4-</sup> anion. However, not all cases are as clear-cut since there may be extensive mixing of M–M and M–ligand bonding such that the significance and validity of an M–M bond order or its assignment is questionable.

The formal bond order which depends only on a qualitative electron count, as deduced from the formal oxidation state of the metal atoms, therefore overlooks the possibility of M–M, M–L (axial and/or equatorial) mixing or the effect of torsional twist about the M–M bond on the  $\delta$  component of the quadruple bond.

The dichromium(II) compounds are all formally quadruple in order. However, the large variation in Cr–Cr distance raises the question as to whether these bonds can reasonably be

† Present address: ISCOR Head Office, Research and Development, P.O. Box 450, Pretoria 0001, South Africa.

<sup>®</sup> Abstract published in *Advance ACS Abstracts*, March 1, 1995.

(1) Cotton, F. A.; Wang, W. *Nouv. J. Chem.* **1984**, 8, 331.

(2) Boeyens, J. C. A.; Cotton, F. A.; Han, S. *Inorg. Chem.* **1985**, 24, 1750.

(3) Boeyens, J. C. A.; *Inorg. Chem.* **1985**, 24, 4149.

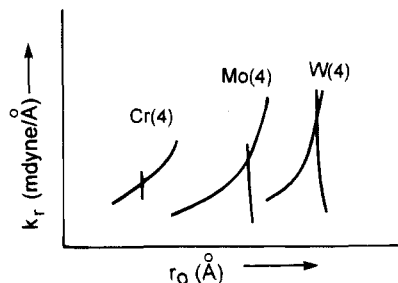


**Figure 1.** Schematic drawing to illustrate the crossing of solution curves  $\{k, r_0\}$  for bonds of the same order but different steric environments.

considered to be of the same order. The large differences indicate that behind the formal concept of quadruple bonding the real bonding situation may be quite different. The axial and equatorial ligands could, for instance, have a decisive influence on the electron density at the dimetal center.

Likewise, the dimolybdenum(II) bonds are all formally quadruple. However,  $\delta$  overlap is angle sensitive. Nonbonded repulsions between the sets of ligands at the two ends of a  $X_4M_2-(L^A L)_2$  unit, should favor rotation away from the eclipsed conformation, and only a limited amount of twist can occur without loss of the  $\delta$  contribution. Also, the  $\delta$  bonding depends on lateral overlap of the  $d\delta$  orbitals, a type of overlap that diminishes rapidly as the internuclear distance increases. The effective bond order of a dimetal center may thus not depend only on the number of electrons formally available for M–M bond formation but also on the ligand environment.

To analyze the situation by molecular mechanics, a dimetal system with definite bond orders is needed as a model. Since the formally quadruple Mo–Mo unit appears to be structurally rigid with relatively slight variations in the M–M distance due to the influence of the ligand environment, and because of the available range of bond orders structurally characterized, this system will serve as the model for our study of the dichromium bond through molecular mechanics.

### Transferable Force-Field Parameters

A fundamental assumption of molecular modeling is the transferability of force-field parameters between equivalent bonds in different environments. In the case of the dimetal center, this implies a unique pair  $(k, r_0)$  for a fixed bond order. The possibility of generating noncoincident solution curves  $\{k, r_0\}$  for a bond of given order in sterically different environments therefore exists. This strategy has in fact been proven feasible for the quadruple bonds in  $Cr_2$ ,  $Mo_2$ , and  $W_2$ , by comparing bridged and unbridged dimetal centers of the types  $M_2(X^A Y)_4$  and  $M_2(CH_3)_8^{4-}$ , respectively.<sup>3</sup> The solution curves reproduced as Figure 1 are seen to have positive slopes for the unbridged and negative slopes for the bridged compounds.

The points of intersection can immediately be interpreted as defining the unique pair,  $(k, r_0)$ , for each quadruple bond. As a final validation of the scheme, the relative stabilities of staggered and eclipsed conformations of the unbridged compounds were compared by driving a rotation around the dimetal bond and analyzing the steric strain as a function of rotation angle. To stabilize the known eclipsed conformations, an electronic stabilization corresponding well with the theoretical  $\delta$  contribution was required.

A similar analysis can now be envisaged for all other bond orders so as to establish a general relationship among  $k_r$ ,  $r_0$ , and bond order,  $N$ . A useful representation of such a relationship for some dimetal center would be graphical variation of  $k_r$  vs  $r_0$  for all bond orders, as shown in Figure 2. Points on the

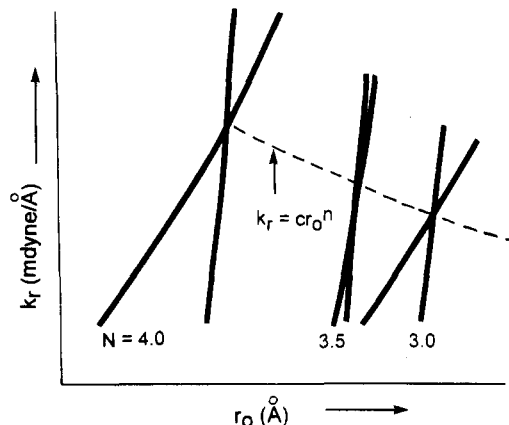


**Figure 2.** Schematic drawing of intersecting solution curves at different bond orders and the functional relationships between the solution pairs  $(k, r_0)_N$ .

curve satisfy three relationships:

$$k_r = cr_0^n \quad (1)$$

$$N = bk_r^m \quad (2)$$

$$N = bc^m r_0^{nm} \quad (3)$$

where the coefficients and powers are to be established empirically. The first relationship will be the practically most useful one, as a sampling curve to derive bond orders from a family of solution curves  $\{k, r_0\}$ , for a variety of compounds with a common dimetal center. Only then can the problem of variability in bond length, as observed for dichromium systems, be analyzed systematically. Should the variability be linked to a variation in bond order, final confirmation should come from observed barriers to rotation.

The grand aim of this study is therefore to identify a sufficient number of compounds of authentic bond order over the entire range, to enable the construction of a sampling curve for each homonuclear dimetal system of periodic group 6. It is assumed that the same force law applies to yield characteristic coefficients ( $c$ ,  $b$ ) for each metal. Periodic variation of  $b$  and  $c$  should define some trend, such as an index of flexibility. The only criterion limiting the inclusion of specific molecules into the sample is a known crystal structure, without disorder. In practice, this limitation is severe for  $Cr_2$  and  $W_2$  compounds. In the case of dichromium, it is because of the very problem that we hope to solve, viz. the uncertainty about the bond order of most compounds. For ditungsten, it is simply a dearth of reported structures. As a consequence, dimolybdenum systems have been modeled in large numbers and detail, not only to establish a reliable sampling curve for this family but also to enable extrapolation to dichromium with its insufficient population of compounds from a single fixed point on the sampling curve.

The results were of sufficient quality to establish a dichromium sampling curve, fully consistent with other experimental evidence like the  $\delta$  contribution to the bonding and observed properties of single-bond dichromium. Only the results for dimolybdenum quadruple bonds are presented here.

Compared to that of dichromium, the central bond in dimolybdenum compounds of the type  $L_4Mo-MoL_4$ , is remarkably robust and insensitive to the nature of both equatorial and axial ligands. It can therefore be assumed with a fair degree of confidence that the dimetal bond order would only depend on the number of electron pairs formally associated with formation

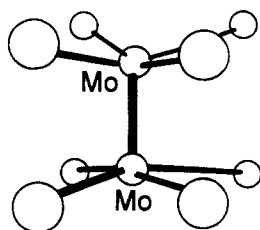


**Figure 3.** Perspective drawing of the general eclipsed dimetal system without bridging ligands.

of the bond. For the Mo(II) oxidation state, these bonds should therefore be of order 4 and ground state  $\sigma^2\pi^4\delta^2$ .

To model this bond in molecular mechanics, it is necessary to know either the harmonic force constant,  $k_r$ , or the characteristic bond length,  $r_0$ , as determined by electronic factors only. The second, unknown parameter can then be varied until the crystallographically known bond length and the correct molecular conformation are reproduced in terms of the minimized steric energy with bonding contribution,  $V(r) = \frac{1}{2}k_r(r - r_0)^2$ .

Should neither  $k_r$  nor  $r_0$  be known, a range of values for either can be chosen and for each choice the matching second parameter can be established as the value that reproduces the known structure as before, to yield a set of solution pairs ( $k_r$ ,  $r_0$ ). A solution curve  $\{k_r, r_0\}$  is thus constructed for each Mo<sub>2</sub> bond that occurs in a compound of known crystal structure. This method will now be applied to all known Mo<sup>4</sup>–Mo bonds. Since the Mo<sub>2</sub> units occur in different environments, the solution curves should in general not be coincident. The slopes of the solution curves are specifically expected to be different for ligand-bridged and unbridged bonds, respectively. A general point of intersection would then uniquely establish the pair ( $k_r$ ,  $r_0$ ) that corresponds to the true transferable properties of the Mo<sub>2</sub> bond.

Only crystallographically well-refined structures are included in the analysis. In many cases it was necessary to generate hydrogen and lone-pair coordinates geometrically. The estimated standard deviations associated with all optimized structures do not exceed 0.1 Å for bond lengths, 3° for bond angles, and 5° for out-of-plane bends and torsions.

### The Unbridged Compounds

Unbridged dimolybdenum compounds with crystallographically known structures are essentially of two types: the [Mo<sub>2</sub>X<sub>8</sub>]<sup>4-</sup> ions with essentially eclipsed  $D_{4h}$  conformation and Mo<sub>2</sub>X<sub>4</sub>(PR<sub>3</sub>)<sub>4</sub> molecules with  $D_{2d}$  eclipsed geometry. Both types have the general arrangement of ligands shown in Figure 3. The observed Mo–Mo–X angles are in the range 105–116°, the observed Mo–Mo–P angles are 98–105°, the X–Mo–X angles are 85–87°, and the X–Mo–P angles are 82–89°. The structures are therefore modeled as two square planar MoL<sub>4</sub> units, linked by an Mo–Mo bond.

The force field is summarized in Tables 1–3 and incorporates a special procedure for torsional interaction described in the Appendix. Each of the Cl, Br, and Me ligands in [Mo<sub>2</sub>X<sub>8</sub>]<sup>4-</sup> carries a charge of  $-1/2$ , and their Coulombic repulsion is included in the computation of the minimized structure. To ensure the planarity of phenyl rings, 1,4(C–C)<sub>ar</sub> interaction is treated as a bond rather than a nonbonded interaction and out-of-phase ( $\delta$ ) movement of aromatic hydrogen atoms is constrained according to  $V(\delta) = \frac{1}{2}k_\delta(\delta - \delta_0)^2$ , using  $k_\delta = 0.29$  mdyn Å. Torsional interaction in the aromatic system is

**Table 1.** Harmonic Bond-Deformation Force-Field Parameters Used in This Study

bond	$k_r$ /mdyn Å <sup>-1</sup>	$r_0$ /Å	bond	$k_r$ /mdyn Å <sup>-1</sup>	$r_0$ /Å
Mo–Cl <sup>(1/2)-</sup>	0.70	2.35	C–H	5.00	1.08
Mo–Br <sup>(1/2)-</sup>	0.70	2.52	(C–H) <sub>ar</sub>	5.00	1.08
Mo–C <sup>(1/2)-</sup>	1.98	2.27	C≡N	3.00	1.15
Mo–P	0.70	2.50	C–N	3.00	1.44
Mo–C	2.00	2.20	(C–N) <sub>br</sub>	3.00	1.30
Mo–Cl	0.70	2.39	(C–N) <sub>ar</sub>	7.65	1.34
Mo–Br	0.70	2.53	para(C–N) <sub>ar</sub>	0.05	2.78
Mo–I	0.70	2.70	C–O	3.00	1.42
Mo–O <sub>br</sub> <sup>a</sup>	0.84	2.07	(C–O) <sub>br</sub>	3.00	1.26
Mo–O <sub>br</sub> (sulfate)	0.90	2.10	C–F	2.00	1.30
Mo–C <sub>br</sub>	1.96	2.14	C–P	3.50	1.80
Mo–N <sub>br</sub>	0.84	2.10	C–S	2.50	1.62
Mo–O <sub>ax</sub> <sup>b</sup>	0.40	2.65	C–Cl	2.00	1.70
(intermolecular)					
Mo–N <sub>ax</sub>	0.80	2.54	C–Br	2.00	1.80
Mo–O <sub>ax</sub> (THF)	0.60	2.50	(N–N) <sub>br</sub>	3.00	1.25
Mo–Cl <sub>ax</sub>	0.20	3.30	N–H	5.00	1.00
Mo–Br <sub>ax</sub>	0.30	3.40	N–Lp	6.00	1.00
Mo–O <sub>s</sub> (sulfate, intermolecular)	0.50	2.57	O–Lp	6.00	1.00
Mo–NCS	0.70	2.00	O=S	3.50	1.44
C–C	5.00	1.54	O–S	3.00	1.50
(C–C) <sub>ar</sub> <sup>c</sup>	7.65	1.39	P–H	5.00	1.25
para(C–C) <sub>ar</sub>	0.05	2.78	P–Lp	6.00	1.00

<sup>a</sup> br = bridging ligand. <sup>b</sup> ax = axial ligand. <sup>c</sup> ar = aromatic.

modeled to be attractive toward  $\chi = 0$ ,  $V_0 = 0.21$  kJ mol<sup>-1</sup>, compared to  $V_{60} = 0.02$  kJ mol<sup>-1</sup> for the normal repulsive torsions.

The  $\delta$  contribution to quadruple bond strength presents an interesting problem that can be solved directly by molecular mechanics. The torsional interaction across the dimetal bond is replaced by an artificial incremental parameter that allows the program<sup>7</sup> to drive the rotation around the bond, while sampling the equilibrium steric strain at each position.

The results for three Mo<sub>2</sub>X<sub>8</sub><sup>4-</sup> ions are shown in Figure 4. The steric energy has a maximum for the eclipsed structures ( $\chi = 0$ ) in all cases. This means that the observed structure can only be stabilized by an electronic interaction not included in the calculated steric energy. This is the  $\delta$  contribution. For [Mo<sub>2</sub>Me<sub>8</sub>]<sup>4-</sup> local minima occur at  $\chi = 30$  and  $60^\circ$  rather than  $45^\circ$ . This was explained before<sup>3</sup> in terms of the 3-fold symmetry of the methyl groups, superimposed on the overall 4-fold symmetry. The potential energy difference between the maxima and the minima amounts to  $\Delta U = 31.4, 46.0$ , and  $48.1$  kJ mol<sup>-1</sup> for X = Me, Cl, and Br, respectively, and defines a lower limit to the  $\delta$  contribution. Other, independent estimates yielded 62.8 kJ/mol<sup>8</sup> and 41.4 kJ/mol<sup>2</sup>, in good agreement with the present result.

Using attractive  $\delta$  torsion potentials, sufficient to overcome the steric repulsion, in the force field already defined, allowed the calculation of the  $\{k_r, r_0\}$  solution curves, shown in Figure 5 for the 10 unbridged dimolybdenum compounds listed in Table 4. The calculated Mo–Mo distances produced by all pairs ( $k_r, r_0$ ) along the solution curves, all correspond to within 0.001 Å with

(4) Scott, R. A.; Scheraga, H. A. *J. Chem. Phys.* **1965**, *42*, 2209.

(5) Pitzer, K. S. *Adv. Chem. Phys.* **1959**, *2*, 367.

(6) Ketelaar, J. *Chemical Constitution*; Elsevier: Amsterdam, 1953.

(7) Boyd, R. H. *J. Chem. Phys.* **1968**, *49*, 2574.

(8) Hopkins, M. D.; Zietlow, T. C.; Miskowski, V. M.; Gray, H. B. *J. Am. Chem. Soc.* **1985**, *107*, 510.

(9) Cotton, F. A.; Troup, J. M.; Webb, T. R.; Williamson, D. H.; Wilkinson, G. *J. Am. Chem. Soc.* **1974**, *94*, 3824.

(10) Cotton, F. A.; Wiesinger, K. *J. Inorg. Chem.* **1990**, *29*, 2594.

(11) Cotton, F. A.; Daniels, L. M.; Powell, G. L.; Kahaian, A. J.; Smith, T. J.; Vogel, E. F. *Inorg. Chim. Acta.* **1988**, *144*, 109.

(12) Brencic, J. V.; Cotton, F. A. *Inorg. Chem.* **1969**, *8*, 7.

(13) Brencic, J. V.; Leban, I.; Segedin, P. Z. *Anorg. Allg. Chem.* **1976**, *427*, 85.

Table 2. Harmonic Angle-Bending Parameters

angle	$k_{\theta}/\text{mdyn } \text{\AA} \text{ rad}^{-1}$	$\theta_0/\text{rad}$	angle	$k_{\theta}/\text{mdyn } \text{\AA} \text{ rad}^{-1}$	$\theta_0/\text{rad}$
Mo-Mo-L <sub>ax</sub> <sup>a</sup>	0.30	3.1416	(X/Y) <sub>br</sub> -Z <sub>br</sub> -L <sub>p</sub>	0.60	2.094
Mo-Mo-L <sub>br</sub>	0.20	1.571	X <sub>br</sub> -Z <sub>br</sub> -Y <sub>br</sub>	1.50	2.094
Mo-Mo-Cl <sup>(1/2)-</sup>	0.60	1.571	(X/Y) <sub>br</sub> -Z <sub>br</sub> -(C/H)	1.00	2.094
Mo-Mo-Br <sup>(1/2)-</sup>	0.70	1.571	L <sub>ar</sub> -L <sub>ar</sub> -L <sub>ar</sub> <sup>e</sup>	1.00	2.094
Mo-Mo-C <sup>(1/2)-</sup>	0.70	1.571	L <sub>ar</sub> -L <sub>ar</sub> -L	0.65	2.094
Mo-Mo-C	0.10	1.571	Z <sub>br</sub> -(X/Y) <sub>br</sub> -L	0.20	2.094
Mo-Mo-P	0.30	1.571	C-C-(C/O)	0.10	1.911
Mo-Mo-Hal <sup>b</sup>	0.10	1.571	C-C-(H/F)	0.65	1.911
Mo-Mo-N	0.10	1.571	F-C-F	0.52	1.911
Cl <sup>(1/2)-</sup> -Mo-Cl <sup>(1/2)-</sup>	0.50	1.571	X-C-H	0.65	1.911
Br <sup>(1/2)-</sup> -Mo-Br <sup>(1/2)-</sup>	0.50	1.571	H-C-X	0.10	1.911
C <sup>(1/2)-</sup> -Mo-C <sup>(1/2)-</sup>	0.60	1.571	H-C-H	0.52	1.911
P-Mo-C	0.10	1.571	P-C-H	0.65	1.911
Hal-Mo-P	0.10	1.571	(C-C-C) <sub>ar</sub>	1.00	2.094
L <sub>ax</sub> -Mo-L <sub>br</sub>	0.80	1.571	C <sub>ar</sub> -C <sub>ar</sub> -(H <sub>ar</sub> /P)	0.65	2.094
X <sub>br</sub> -Mo-Y <sub>br</sub> <sup>c</sup>	0.80	1.571	(C-C-P) <sub>br</sub>	0.60	1.911
P-Mo-N	0.10	1.571	P <sub>br</sub> -C <sub>br</sub> -P	0.20	1.911
Mo-O <sub>br</sub> -L <sub>p</sub>	0.40	2.094	P <sub>br</sub> -C <sub>br</sub> -C	0.10	1.911
Mo-(X/Y) <sub>br</sub> -Z <sub>br</sub>	0.20	2.094	N≡C-S	0.30	3.1416
Mo-O <sub>br</sub> -C	0.20	2.094	(P-C-P) <sub>br</sub>	0.60	1.911
Mo-N <sub>br</sub> -H	0.40	2.094	Y <sup>f</sup> -O-L <sub>p</sub>	0.40	1.911
Mo-N <sub>br</sub> -C <sub>ar</sub>	0.20	2.094	C-O-C	0.20	1.911
Mo-O <sub>ax</sub> -C	0.20	2.094	C-O-C	0.10	2.094
Mo-P <sub>br</sub> -C <sub>br</sub>	0.10	1.911	C-P-L <sub>p</sub>	0.40	1.911
Mo-N≡C	0.30	3.1416	C-P-C/C <sub>ar</sub>	0.10	1.911
Mo-X <sub>ar</sub> -C <sup>d</sup>	0.20	1.911	C <sub>ar</sub> -P-H	0.65	1.911
Z-(X/Y)-(H/L <sub>p</sub> )	0.60	2.094	O <sub>br</sub> -S <sub>br</sub> =O	1.00	1.911

<sup>a</sup> L = H<sub>ar</sub>, O<sub>br</sub>, C, N<sub>br</sub>, F, Cl, C<sub>ar</sub>, Mo. <sup>b</sup> Hal = halogen. <sup>c</sup> X<sub>br</sub>, Y<sub>br</sub>, Z<sub>br</sub> = C<sub>br</sub>, N<sub>br</sub>, O<sub>br</sub>. <sup>d</sup> X = Cl, Br, O. <sup>e</sup> L<sub>ar</sub> = C<sub>ar</sub>, N<sub>ar</sub>. <sup>f</sup> Y = C, L<sub>p</sub>, S<sub>br</sub>.

observed values. The solution curves are clustered sufficiently ( $\Delta r_0 = 0.02 \text{ \AA}$ ) to show that the bond orders are essentially the same. The positive slopes indicate<sup>3</sup> stretching of the dimetal bond by steric factors.

A reassuring feature of the analysis was the way in which all structural variations, often unexpected, like the shorter Mo-Mo bond in Mo<sub>2</sub>Br<sub>8</sub><sup>4-</sup> compared to Mo<sub>2</sub>Cl<sub>8</sub><sup>4-</sup>, were faithfully reproduced in the simulations.

### Bridged Compounds

A large number of dimolybdenum-bridged compounds with the familiar paddle-wheel shape are known. They belong to two general classes, Mo<sub>2</sub>(X-Z-Y)<sub>4</sub> and Mo<sub>2</sub>(X-Z-Y)<sub>4</sub>L<sub>2</sub>, where L is an axial ligand and X<sup>^</sup>Y most commonly represents O<sup>^</sup>O, N<sup>^</sup>O, and N<sup>^</sup>N bridges. The molecular shape is illustrated in Figure 6. In molecular mechanics the L-free compounds are treated as two square planar Mo(X<sub>2</sub>Y<sub>2</sub>) units, linked by the dimetal bond, and the fully substituted compounds are treated as an octahedral arrangement of X<sub>2</sub>Y<sub>2</sub>LMo around each molybdenum atom.

Within a given class of bridging ligands, all molecular dimensions, besides the Mo-Mo bond, are statistically indistinguishable since the supporting framework is comparatively insensitive to changes in dimetal bond length. The framework for given X-Z-Y is therefore simulated by a transferable force field. Lone pairs are treated as hydrogen atoms in nonbonded interactions. Their behavior in all other situations is defined in the Tables 1-3.

The structure of [Mo<sub>2</sub>(SO<sub>4</sub>)<sub>4</sub>]<sup>4-</sup> which falls in the present class was successfully modeled without consideration of Coulombic interactions. The half charges, located on the outermost oxygen atoms, have no influence on the central Mo<sub>2</sub>O<sub>8</sub> core. Unlike all other X-Z-Y bridges, the Mo<sub>2</sub>O<sub>2</sub>S rings are nonplanar and

have a dihedral bend of 20° across the O---O line. Torsional interactions across the ligand-ligand and metal-ligand bonds are thus attractive for (C-C)<sub>ar</sub>, (C<sub>ar</sub>-N), and (X,Y)-Z, provided Z ≠ S. V<sub>0</sub> = 0.21 kJ mol<sup>-1</sup>. For all other twists a repulsion of V<sub>60</sub> = 0.02 kJ mol<sup>-1</sup> operates. Constraints were placed again on the angular movement ( $\delta$ ) of the atoms (H, O, C, Cl, Mo, F) bound to C<sub>ar</sub> and N<sub>ar</sub>, out of the phenyl ring plane,  $k_{\delta} = 0.29 \text{ mdyn } \text{\AA}$ .

Allowing for delocalization in the Mo<sub>2</sub>XZY ring is equivalent to the  $\delta$ -bond parameter introduced before to ensure an eclipsed unbridged structure. Although this factor is absent for sulfato bridges, eclipsing in this case is sterically enforced. Modeling of the isostructural, triply bonded Mo<sub>2</sub>(HPO<sub>4</sub>)<sub>4</sub>L<sub>2</sub> molecules (to be described in a later paper) shows an eclipsed conformation to be favored in the absence of any  $\delta$  bonding. This emphasizes that eclipsing does not imply  $\delta$  bonding but that  $\delta$  bonding demands an eclipsed structure.

Solution curves for 24 compounds listed in Table 5 were generated by matching the MM-minimized arrangements with crystallographically determined structures, using the same

- (14) Hopkins, M. D.; Schaefer, W. P.; Bronikowski, M. J.; Woodruff, W. H.; Miskowski, V. M.; Dallinger, R. F.; Gray, H. B. *J. Am. Chem. Soc.* **1987**, *109*, 408.  
 (15) Cotton, F. A.; Extine, M. W.; Felthouse, T. R.; Kolthammer, B. W. S.; Lay, D. G. *J. Am. Chem. Soc.* **1981**, *103*, 4040.

- (16) Kelley, S. N.; Fink, M. *J. Chem. Phys.* **1982**, *76*, 1407.  
 (17) Cotton, F. A.; Thompson, J. L. *Inorg. Chem.* **1981**, *20*, 3887.  
 (18) Cotton, F. A.; Feng, X.; Matusz, M. *Inorg. Chem.* **1989**, *28*, 584.  
 (19) Cotton, F. A.; Rice, G. W.; Sekutowski, J. C. *Inorg. Chem.* **1979**, *18*, 1143.  
 (20) Cotton, F. A.; Isley, W. H.; Kaim, W.; *Inorg. Chem.* **1980**, *19*, 1453.  
 (21) Bino, A.; Cotton, F. A.; Kaim, W. *Inorg. Chem.* **1979**, *18*, 3030.  
 (22) Cotton, F. A.; Koch, S. A.; Millar, M. *Inorg. Chem.* **1978**, *17*, 2087.  
 (23) Cotton, F. A.; Fanwick, P. E.; Niswander, R. H.; Sekutowski, J. C. *J. Am. Chem. Soc.* **1978**, *100*, 4725.  
 (24) Cotton, F. A.; Niswander, R. H.; Sekutowski, J. C. *Inorg. Chem.* **1979**, *18*, 1152.  
 (25) Cotton, F. A.; Isley, W. H.; Kaim, W. *Inorg. Chem.* **1980**, *19*, 3586.  
 (26) Cotton, F. A.; Niswander, R. H.; Sekutowski, J. C. *Inorg. Chem.* **1978**, *17*, 3541.  
 (27) Cotton, F. A.; Isley, W. H.; Kaim, W. *J. Am. Chem. Soc.* **1980**, *102*, 3475.  
 (28) Baral, S.; Cotton, F. A.; Isley, W. H. *Inorg. Chem.* **1981**, *20*, 2696.  
 (29) Baral, S.; Cotton, F. A.; Isley, W. H.; Kaim, W. *Inorg. Chem.* **1982**, *21*, 1644.  
 (30) Cotton, F. A.; Norman, J. G.; Stults, B. R.; Webb, T. R. *J. Coord. Chem.* **1976**, *5*, 217.

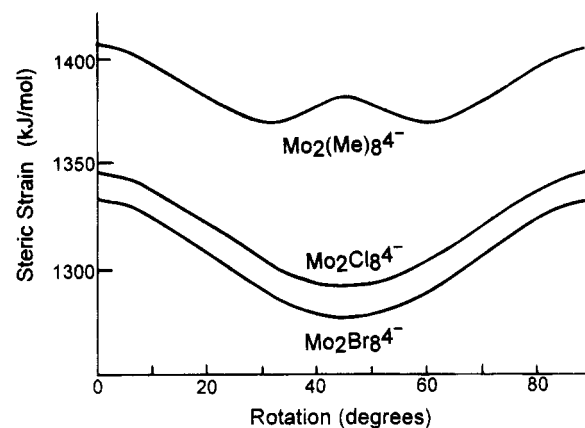
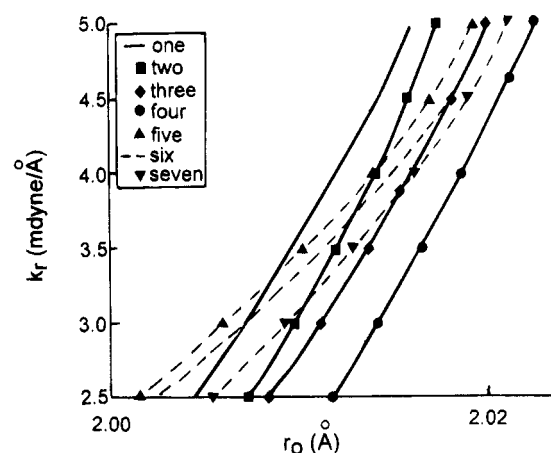
**Table 3.** Parameters for the Nonbonded Potential  $V_{ij} = a \exp(-br_{ij}) - c/(r_{ij})^6$ <sup>a</sup>

interaction	$a/10^5 \text{ kJ mol}^{-1}$	$b/\text{\AA}^{-1}$	$c/10^2 \text{ \AA}^6 \text{ kJ mol}^{-1}$
Mo---Mo	0.6645	2.60	39.76
Mo---H	0.9218	3.44	7.712
Mo---C	4.634	3.46	22.89
Mo---N	3.242	3.46	23.02
Mo---O	3.792	3.47	23.68
Mo---F	1.772	3.47	13.98
Mo---P	4.361	3.20	48.44
Mo---S	3.838	3.16	54.59
Mo---Cl	3.137	3.12	61.45
Mo---Br	1.063	2.69	87.96
Mo---I	1.134	2.55	136.8
H---H	1.056	4.55	2.067
H---C	5.313	4.57	5.495
H---N	3.336	4.58	5.362
(H,Lp)---O	3.742	4.58	5.362
(H,Lp)---F	1.486	4.59	2.784
(H,Lp)---P	5.415	4.24	11.03
(H,Lp)---S	2.289	3.94	13.13
H---Cl	3.625	4.13	14.16
H---Br	1.383	3.56	20.48
H---I	1.600	3.38	31.69
C---C <sup>b</sup>	30.35	4.60	15.24
C---N <sup>b</sup>	17.97	4.60	15.00
C---O	21.25	4.61	15.18
C---F	8.320	4.61	8.194
C---P	28.71	4.26	31.09
C---S	13.13	4.05	32.41
C---Cl	18.20	4.15	39.82
C---Br	6.242	3.58	57.42
C---I	7.115	3.40	89.17
N---N	11.33	4.61	14.88
N---O	13.52	4.61	15.79
N---F	5.600	4.62	8.616
N---P	18.62	4.27	30.85
N---S	15.58	4.21	34.88
N---Cl	12.85	4.16	41.45
N---Br	4.657	3.58	59.71
O---O	15.18	4.62	15.24
O---F	4.164	4.62	8.435
O---S	10.12	4.18	27.71
O---Cl	13.73	4.16	39.95
O---Br	4.86	3.58	57.48
F---F	2.73	4.63	4.910
P---P	28.10	3.95	63.86
P---S	24.05	3.90	72.30
P---Cl	18.74	3.85	81.94
P---Br	6.519	3.32	118.1
P---I	7.260	3.15	182.6
S---S	17.77	3.80	84.43
Cl---Cl	13.05	3.75	104.8
Br---Br	2.002	2.79	216.9
I---I	2.443	2.51	521.8

<sup>a</sup> The constant  $a$  is obtained by minimization of  $V_{ij}$  at  $r_{ij} = r_i + r_j$ , the sum of the van der Waals radii;  $b$  is a shielding factor; <sup>4</sup> and  $c$  is a function of steric polarizabilities and valence electron densities<sup>4-6</sup>.

<sup>b</sup> The same parameters apply for aromatic systems except for 1,4 interactions with  $V = 0$ .

convergence criteria as for the unbridged compounds. The solution curves are shown in Figure 7. They clearly separate into two sets with somewhat different slopes. The solid curves

**Figure 4.** Angular variation of steric strain in quadruply bonded  $[\text{Mo}_2\text{X}_8]^{4-}$  ions.**Figure 5.** Molecular mechanics solution curves  $\{k_r, r_0\}$  for the unbridged dimolybdenum center of order 4.**Table 4.** Calculated and Observed Dimetal Bond Lengths in Unbridged Dimolybdenum Moieties

formula	obs/\AA	calc/\AA	figure label	ref
$[\text{Mo}_2\text{Me}_8]^{4-}$	2.148(2)	2.148	three	9
$\text{Mo}_2\text{Me}_4(\text{PMe})_4$	2.1489(4)	2.149	one	10
$\text{Mo}_2\text{Cl}_4(\text{PPh}_2)_4$	2.1474(9)	2.149	one	11
$[\text{Mo}_2\text{Cl}_8]^{4-}$	2.138(3)	2.136	six	12
$[\text{Mo}_2\text{Br}_8]^{4-}$	2.135(2)	2.135	six	13
$\text{Mo}_2\text{Br}_4(\text{PMe}_3)_4$	2.125(1)	2.126	four	14
$\text{Mo}_2\text{I}_4(\text{PMe}_3)_4$	2.127(1)	2.126	four	14
$\text{Mo}_2\text{Cl}_4(\text{PMe}_2\text{Ph})_4$	2.1288(8)	2.129	five	11
$\text{Mo}_2\text{Cl}_4(\text{PMe}_3)_4$	2.130(1)	2.130	five	15
$\text{Mo}_2\text{Me}_4(\text{PMe}_2\text{Ph})_4$	2.164(1)	2.164	two	10

represent all those compounds without axial ligands and those with weakly donating axial ligands like  $\text{CH}_2\text{Cl}_2$  and  $\text{CH}_2\text{Br}_2$ . All the others are represented by the broken curves. The clustering of the curves is such as to indicate a common bond order for all compounds involved, significantly including those with strongly donating axial ligands.

### Twisted Bridges

Although bridged compounds with an  $\text{M}^4\text{--M}$  bond prefer an eclipsed arrangement, for one reason or the other, bulky substituents could distort this through steric interaction. This happens with phosphine bridges of the type  $\text{R}_2\text{P--C}_n\text{--PR}_2$ , and the interesting question is the degree of twist that can be tolerated without destroying the  $\delta$  interaction.

Many interesting structures in this family are unfortunately disordered<sup>38</sup> and therefore not considered in this analysis. In at least one case<sup>39</sup> molecules do occur with different geometries

- (31) Cotton, F. A.; Mester, Z. C.; Webb, T. R. *Acta Crystallogr.* **1974**, B30, 2768.  
 (32) Cotton, F. A.; Extine, M.; Gage, C. D. *Inorg. Chem.* **1978**, 17, 172.  
 (33) Cotton, F. A.; Norman, J. G. *J. Coord. Chem.* **1971**, 1, 161.  
 (34) Cotton, F. A.; Falvello, L. R.; Han, S.; Wang, W. *Inorg. Chem.* **1983**, 22, 4106.  
 (35) Angell, C. L.; Cotton, F. A.; Bertram, A. F.; Webb, T. R. *J. Chem. Soc., Chem. Commun.* **1973**, 399.  
 (36) Cotton, F. A.; Bertram, A. F.; Pederson, E.; Webb, T. R. *Inorg. Chem.* **1975**, 14, 391.  
 (37) Cotton, F. A.; Norman, J. G. *J. Am. Chem. Soc.* **1972**, 94, 5967.

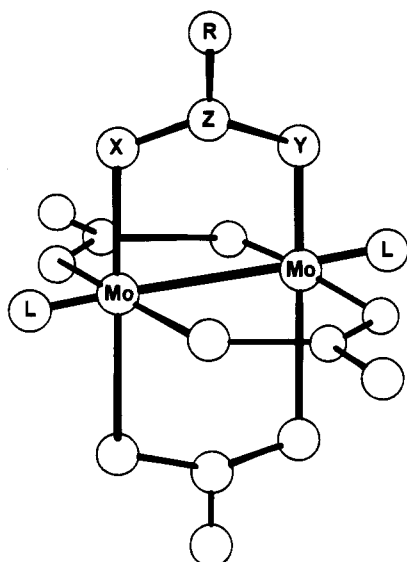


Figure 6. Perspective drawing of the  $\text{Mo}_2(\text{X}-\text{Y}-\text{Z})\text{L}_2$  class of bridged compounds.

Table 5. Calculated and Observed Dimetal Bond Lengths in Compounds  $\text{Mo}_2(\text{XZY})_4\text{L}_2$

anion (XYZ)	$(\text{Lax})_n$	calc/Å	obs/Å	label (Figure 5)	ref
O-C(Me)-O		2.079	2.079(3)	three	16
O-C(biph)-O		2.082	2.082(1)	four	17
DFM <sup>a</sup>		2.082	2.085(4)	four	18
PhN-N-NPh		2.083	2.083(2)	four	19
CHP <sup>a</sup>		2.083	2.085(1)	four	20
PhN-C(Me)-O		2.083	2.086(2)	four	21
DMP <sup>a</sup>		2.064	2.064(1)	two	22
MHP <sup>a</sup>		2.064	2.065(1)	two	23
DMHP <sup>a</sup>		2.072	2.072(1)	one	24
PhN-C(CMe <sub>3</sub> )-O		2.071	2.070(1)	one	25
MAP <sup>a</sup>		2.071	2.070(1)	one	26
NXA <sup>a</sup>	(CH <sub>2</sub> Cl <sub>2</sub> ) <sub>2</sub>	2.083	2.083(3)	four	27
NXA	(CH <sub>2</sub> Br <sub>2</sub> ) <sub>2</sub>	2.083	2.085(2)	four	28
NXA	(py) <sub>1</sub>	2.100	2.101(1)	five	29
NXA	(4-mepy) <sub>2</sub>	2.100	2.102(1)	five	29
NXA	(THF) <sub>2a</sub>	2.091	2.093(2)	six	29
O-C(H)-O	(inter) <sub>2b</sub>	2.090	2.091(2)	six	30
O-C(Me)-O	(inter) <sub>2</sub>	2.091	2.093(1)	six	31
O-C(CMe <sub>3</sub> )-O	(inter) <sub>2</sub>	2.089	2.088(1)	six	32
O-C(CF <sub>3</sub> )-O	(inter) <sub>2</sub>	2.090	2.090(1)	six	33
FHP <sup>a</sup>	(THF) <sub>1</sub>	2.090	2.092(1)	six	34
O-S(O <sub>2</sub> )-O	(inter) <sub>2</sub>	2.112	2.111(1)	seven	35, 36
NXF <sup>a</sup>	(THF) <sub>2</sub>	2.112	2.113(1)	seven	25
O-C(CF <sub>3</sub> )-O	(py) <sub>2</sub>	2.126	2.129(2)	seven	37

<sup>a</sup> Abbreviations: CHP, 6-chloro-2-hydroxypyridine; DFM, di-*p*-tolylformamide; DMHP, 2,4-dimethyl-6-hydroxypyrimidine; DMP, 2,6-dimethoxyphenyl; FHP, 6-fluoro-2-hydroxypyridine; MAP, 6-methyl-2-aminopyridine; MHP, 6-methyl-2-hydroxypyridine; NXA, *N*-(2,6-dimethylphenyl)acetamido; NXF, *N*-(2,6-dimethylphenyl)formamido; THF, tetrahydrofuran. <sup>b</sup> Although there are no axial ligands, all structures designated (inter)<sub>2</sub> are linked into infinite chains in the solid state, through weak coordination by oxygen atoms of neighbouring molecules.

at different crystallographic sites. This could also be due to unresolved disorder, and only those molecules at the low-symmetry sites have been included here.

These compounds, of general formula  $\text{Mo}_2\text{X}_4(\text{L}^\wedge\text{L})_2$ , are in a sense intermediate between the unbridged and the fully bridged compounds considered before. More importantly, the delocalization that promotes eclipsing of flat chelate rings is now

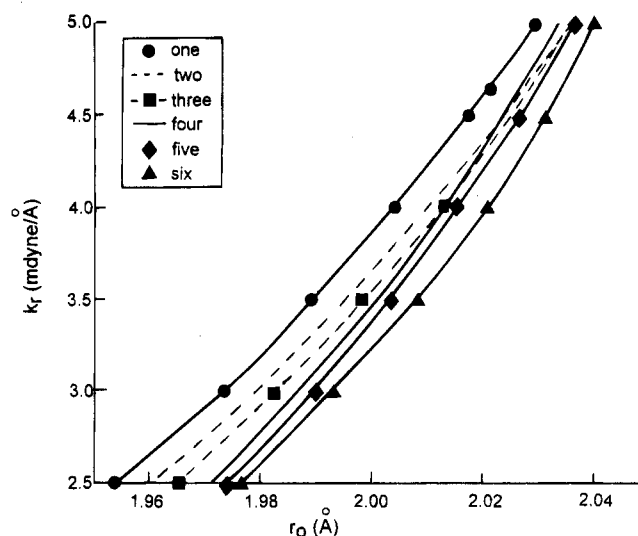


Figure 7. Molecular mechanics solution curves for the  $\text{Mo}_2$  center spanned by bridging ligands.

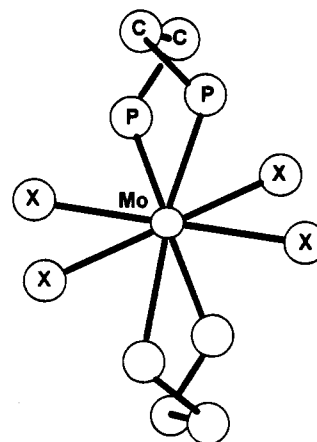


Figure 8. Schematic drawing of a twisted half-bridge structure,  $\text{Mo}_2\text{X}_4-(\text{PCCP})_2$ , viewed down the dimolybdenum axis.

absent. Competition between ring puckering and  $\delta$  bonding therefore occurs. In this connection it is of interest to note that the triply bonded compounds<sup>40</sup>  $\text{Re}_2\text{Cl}_4(\text{dppm})_4$  and  $\text{Re}_2\text{Cl}_4(\text{dppe})_4$  have sterically stabilized<sup>3</sup> staggered conformations.

In order to simulate the observed structures, it is evident that nonzero torsional parameters favoring the eclipsed conformations will be needed. Furthermore, the observed structures represent a balance between rotation around the central bond and steric preference of the coordinated rings. In the case of five-membered rings, as formed by  $\text{Ph}_2\text{P}-\text{CH}_2-\text{PPh}_2(\text{dppm})$  and  $\text{PPh}_2-\text{CH}(\text{PPh})-\text{PPh}_2(\text{tdpm})$ , the P-Mo-Mo-P torsion angles are not equivalent, but for larger rings they are. These include  $\text{PMe}_2-(\text{CH}_2)_2-\text{PMe}_2(\text{dmpe})$ ,  $\text{PPh}_2-(\text{CH}_2)_2-\text{PPh}_2(\text{dppe})$  and  $\text{PPh}_2-(\text{CHMe})_2-\text{PPh}_2(\text{dppb})$ . The structure type is illustrated schematically in Figure 8.

The results of the structure simulations are shown in Table 6. In each case a specific attractive torsional potential was required for successful simulation of the observed conformation. These values are different from the minimum contributions to  $\delta$  interactions, obtained in the analysis of the unbridged structures, and represent the residual interaction at the observed mean angle of rotation. The values decrease as a function of twist angle and represent the extent to which  $\delta$  bonding still operates at each rotation. This empirical torsional potential is seen to be simply related to the mean angle of twist,  $V(\chi) = V_0 \cos 2\chi$ , whereby  $V_0 = 50.0$  kJ/mol. This is an important result. It represents the total  $\delta$  contribution to the rotational

(38) Cotton, F. A.; Powell, G. L. *Inorg. Chem.* **1983**, 22, 1507.

(39) Fanwick, P. E.; Harwood, W. S.; Walton, R. A. *Inorg. Chim. Acta.* **1986**, 122, 7.

**Table 6.** Observed and Calculated Torsion Angles and Parameters across Mo<sub>2</sub> in Twisted-Bridge Compounds<sup>a</sup>

X <sub>4</sub> (P-C <sub>n</sub> -P) <sub>2</sub>	ref	$\chi(\text{P-Mo-Mo-P})$		$\chi(\text{X-Mo-Mo-X})$		$\chi$ deg	$V_0 \cos 2\tilde{\chi}/\text{kJ mol}^{-1}$	$V(\text{obs})/\text{kJ mol}^{-1}$
		obs/deg	calc/deg	obs/deg	calc/deg			
L <sub>4</sub> (dppm) <sub>2</sub>	39	4.9	6	15.6	16	14.35	43.9	44.8
		19.7	21	17.2	17			
(NCS) <sub>4</sub> (dppm) <sub>2</sub>	41	9.0	11	12.0	10	13.33	44.7	44.8
		18.7	16	13.6	14			
Cl <sub>4</sub> (tdpm) <sub>2</sub>	42	10.7	10	21	19	19.78	38.6	41.4
		27.4	26	20	20			
Br <sub>4</sub> (S,S-dppb) <sub>2</sub>	43	-22	-20	-20	-20	21.5	36.6	35.6
		-23	-21	-21	-20			
Cl <sub>4</sub> (S,S-dppb) <sub>2</sub>	43	-24.8	-23	-21.1	-20	24.55	32.7	35.6
		-24.8	-23	-27.5	-26			
L <sub>4</sub> (dppe) <sub>2</sub>	44	-26.5	-28	-25.5	-25	25.6	31.3	31.0
		-26.5	-26	-24	-25			
Br <sub>4</sub> (dmpe) <sub>2</sub>	45	36	38	36	36	36.5	14.6	0
		37	37	37	36			

<sup>a</sup> The parameter for individual torsions is  $V/4$ .  $V_0 = 50$  kJ/mol.

**Table 7.** Calculated and Observed Mo-Mo Bond Lengths in Twist-Bridge Compounds

molecule	calc/Å	obs/Å	label (Figure 6)	$\delta$ -bonding/%
Mo <sub>2</sub> L <sub>4</sub> (dppm) <sub>2</sub>	2.150	2.152(2)	two	88
Mo <sub>2</sub> (NCS) <sub>4</sub> (dppm) <sub>2</sub>	2.165	2.167(3)	one	89
Mo <sub>2</sub> Cl <sub>4</sub> (tdpm) <sub>2</sub>	2.150	2.148(1)	two	77
Mo <sub>2</sub> Br <sub>4</sub> (S,S-dppb) <sub>2</sub>	2.144	2.147(6)	three	73
Mo <sub>2</sub> Cl <sub>4</sub> (S,S-dppb) <sub>2</sub>	2.144	2.147(3)	three	65
Mo <sub>2</sub> L <sub>4</sub> (dppe) <sub>2</sub>	2.180	2.179	four	63

barrier at  $\chi = 0$  and is completely in line with the minima obtained from an analysis of the unbridged Mo<sup>4</sup>-Mo bonds, discussed before.

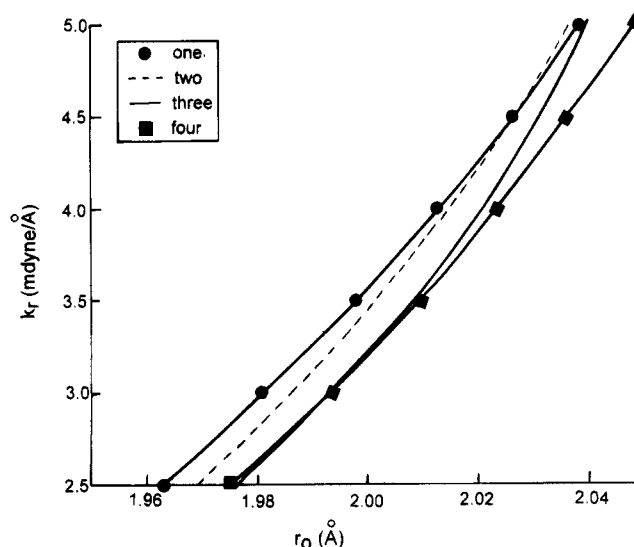
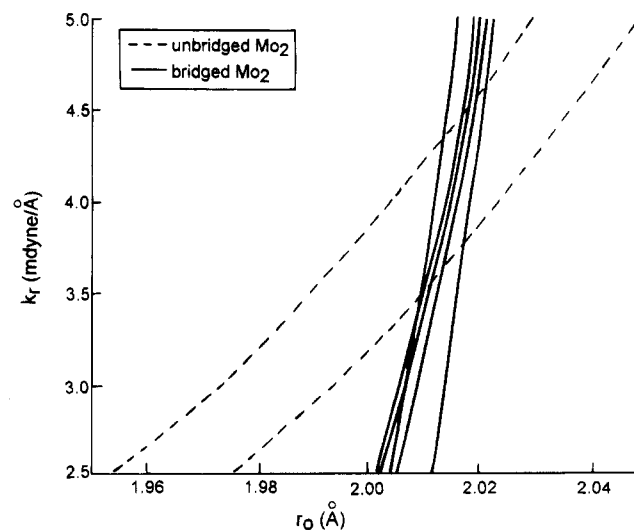
The appropriate parameter for the simulation of the  $\delta$  bonding at any torsion angle  $\chi(\text{Y-Mo-Mo-X})$ , becomes  $V(\chi) = (V_0/4) \cos 2\chi$ . The percentage  $\delta$ -character of a twisted bond follows directly as  $V(\chi)/V_0 = \cos 2\chi$ . The dimetal bond lengths (observed and calculated) are listed in Table 7 to show, in passing, that there is no simple relationship between bond length and twist angle, as surmised before.<sup>38,42</sup>

Solution curves for the twisted dimolybdenum bonds are shown in Figure 9. As expected, all of these are clustered together as for bonds with the same order. The only exception is Mo<sub>2</sub>Br<sub>4</sub>(dmpe)<sub>2</sub>, which, with only 29%  $\delta$ -character, properly belongs with the triple bonds and will not be further considered here.

### The General Solution

Three sets of compounds have now been analyzed to give three sets of solution curves. If they all correspond to a common bond order, the curves should ideally intersect in a single point that represents the solution pair ( $k_r$ ,  $r_0$ ), characteristic of all Mo<sup>4</sup>-Mo bonds. The boundary lines, enveloping all solution curves, for each set, are shown in Figure 10. Intersection occurs in the areas circumscribed by the parameters  $2.01 \leq r_0 \leq 2.02$  Å and  $3.5 \leq k_r \leq 4.64$  mdyn Å<sup>-1</sup>, with average ( $k_r$ ,  $r_0$ ) = (4.07, 2.02).

It is of interest to see how the harmonic force constant derived here compares with spectroscopic data. A summary of experimentally assigned vibration frequencies for dimolybdenum bonds is provided in Table 8. The 4.07 mdyn Å<sup>-1</sup> is in the

**Figure 9.** Molecular mechanics solution curves for the semibridged Mo<sub>2</sub>X<sub>4</sub>(P<sup>^</sup>P)<sub>2</sub> compounds.**Figure 10.** Combined molecular mechanics solution curves  $\{k_r, r_0\}$  for all quadruply bonded Mo<sub>2</sub> compounds.

middle of the observed range 3.17–5.23 mdyn Å<sup>-1</sup>. However, the interpretation is complicated by several factors like anharmonicity, frequency mixing, coupling of modes, diatomic approximation, appropriate reduced mass, resonance enhancement, and, most likely, many more. The best estimate is

(40) Cotton, F. A.; Frenz, B. A.; Ebner, J. R.; Walton, R. A. *Inorg. Chem.* **1976**, *15*, 1630.

(41) Abbot, E. H.; Cotton, F. A. *Inorg. Chem.* **1978**, *17*, 3240.

(42) Campbell, F. L.; Cotton, F. A.; Powell, G. L. *Inorg. Chem.* **1984**, *23*, 4222.

(43) Agaskar, P. A.; Cotton, F. A.; Fraser, I. F.; Peacock, R. D.; *Inorg. Chem.* **1986**, *25*, 2511.



**Table 8.** Experimental Vibration Frequencies and Derived Harmonic Diatomic Force Constants

formula	$\nu^a/\text{cm}^{-1}$	$k/\text{mdyn } \text{\AA}^{-1}$	ref
$\text{Mo}_2(\text{O}_2\text{CCF}_3)_4$	398	4.45	46
$\text{Mo}_2(\text{O}_2\text{CH})_4$	403	4.59	30
$\text{Mo}_2(\text{O}_2\text{CCH}_3)_4$	404	4.61	47
$\text{Mo}_2(\text{O}_2\text{CCF}_3)_4(\text{py})_2$	368	3.83	46
$[\text{Mo}_2(\text{SO}_4)_4]^{4-}$	371	3.89	48
$\text{Mo}_2(\text{MHP})_4$	425	5.11	49
$\text{Mo}_2(\text{CHP})_4$	405	4.64	49
$\text{Mo}_2(\text{FHP})_4\text{THF}$	430 <sup>b</sup>	5.23	34
$[\text{Mo}_2\text{Cl}_8]^{4-}$	350	3.46	50
$[\text{Mo}_2\text{Br}_8]^{4-}$	335	3.17	50
$[\text{Mo}_2\text{Me}_8]^{4-}$	336 <sup>c</sup>	3.19	51
$\text{Mo}_2\text{Cl}_4(\text{PMe}_3)_4$	355	3.56	14
$\text{Mo}_2\text{Br}_4(\text{PMe}_3)_4$	352	3.50	14
$\text{Mo}_2\text{I}_4(\text{PMe}_3)_4$	343	3.33	14

<sup>a</sup> Solid-state Raman spectra. <sup>b</sup> IR solution studies. <sup>c</sup> Solution Raman.

probably the arithmetic average of  $4.04 \text{ mdyn } \text{\AA}^{-1}$ , which corresponds well with the molecular mechanics result.

The present result differs considerably from the preliminary result obtained before<sup>3</sup> from consideration of only two intersecting solution curves. The new value is more reliable, especially in view of the inclusion of Coulombic interaction in the force field, which also resulted in a marked improvement in the match between calculated and observed molecular parameters for the unbridged compounds.

- (44) Cotton, F. A.; Dunbar, K. R.; Matusz, M. *Inorg. Chem.* **1986**, *25*, 3641.  
 (45) Campbell, F. L.; Cotton, F. A.; Powell, G. L. *Inorg. Chem.* **1985**, *24*, 177.  
 (46) San Filipo, J.; Sniadoch, H. J. *Inorg. Chem.* **1973**, *12*, 2326.  
 (47) Hutchinson, B.; Morgan, J.; Cooper, C. B.; Mathey, Y.; Shriver, D. F. *Inorg. Chem.* **1979**, *18*, 2048.  
 (48) Bino, A.; Cotton, F. A.; Marler, D. O. *Inorg. Chim. Acta* **1987**, *133*, 295.  
 (49) Manning, M. C.; Trogler, W. C. *J. Am. Chem. Soc.* **1983**, *105*, 5311.  
 (50) Sattelberger, A. P.; Fackler, J. P. *J. Am. Chem. Soc.* **1977**, *99*, 1258.  
 (51) Bratton, W. K.; Cotton, F. A.; Debeau, M.; Walton, R. A. *J. Coord. Chem.* **1971**, *1*, 121.

## Conclusion

This work has produced the first fixed point in the bond order ( $N$ )—force constant ( $k_r$ )—characteristic bond length ( $r_0$ ) space. The next installment deals with the derivation of further fixed points for the  $\text{Mo}_2$  bonds of orders 3.5, 3, 2, and 1, the functional relationship among all these points, and resolution of the dichromium problem.

## Appendix: The Force Field

The dimetal bond, which often links together eight ligands, differs from the standard aliphatic type that features in most software packages. Instead of a 3-fold barrier to rotation  $\text{M}_2\text{L}_8$  has 4-fold symmetry and a preferred eclipsed, rather than a staggered, conformation. Special allowance is required for this in the force field. The flexible well-tested software of Boyd<sup>7</sup> was adapted for general use in this study. The standard functions for modeling bond stretching, angle bending, out-of-phase bending, and nonbonded and Coulombic interactions were used without modification.

The program calculates all torsional contributions to steric strain from the expression for 3-fold barriers

$$U = \frac{1}{2}V[1 + \cos 3[\chi - (\chi_0 - 180^\circ)]]$$

assuming  $U = 0$  for all  $\chi > 60^\circ$ . Since the total strain is obtained as the sum over all individual contributions, the minimum at  $\chi = 180^\circ$  serves no useful purpose and was suppressed.

The function cannot simulate barriers to rotation about  $\text{L}_4\text{M}-\text{ML}_4$  bonds of order 4 or 3.5 or within delocalized systems. Here it is electronic attraction rather than repulsion that favors eclipsed conformations. A 1-fold torsional potential with a minimum at  $\chi_0 = 0$  was therefore introduced as

$$U_{\chi_0} = \frac{1}{2}V_{\chi=0^\circ}[1 + \cos(|\chi| - b)]$$

where the phase shift,  $b = \chi_0 - 180^\circ$  and  $V_0$  is the torsional potential for pairwise interaction. For  $\text{L}_4\text{M}-\text{ML}_4$  dimers with bond orders of 3 or less, a repulsion that favors  $\chi_0 = 45$  operates.

IC9312704